Model of nuclear excitation by electronic motion in intense laser fields

F. X. Hartmann* and D. W. Noid
Chemistry Division, Oak Ridge National Laboratory, Oak Ridge, Tennessee 37831-6182

Y. Y. Sharon†
Physics Department, Princeton University, Princeton, New Jersey 08544

(Received 28 September 1990; revised manuscript received 10 April 1991)

A simple model of coupled electronic and collective nuclear motion is used to study energy-transfer processes in the presence of intense short-wavelength laser fields. The complete Hamiltonian of the model includes distinct nuclear, electronic, and laser-field terms. A semiclassical method of extracting spectral information from the generated trajectories of the Hamiltonian is used to calculate laser-electronic-nuclear energy-transfer rates. The nuclear term describes a deformed heavy nucleus; it sufficiently treats the collective nuclear motion, which is lower in frequency than that which would be given by an individual-particle nucleon model. We specifically report on the dynamics of this model, and on the energy transfers that ensue, in the presence of an x-ray laser field, as a function of the electron radial distance. This general problem is of basic interest in the studies of laser-driven nuclear excitation.

I. INTRODUCTION

Interactions between the electronic transitions of an atom and the nuclear transitions of its nucleus are of potential importance, both in the excitation of nuclei from ground states to low-lying excited states and in the excitation of short-lived states from long-lived nuclear isomeric states. Such nuclear excitations are shown schematically in Fig. 1.

Part of the initial motivation for the recent work [1–3] in this field by a number of research groups evolved from their interest in investigating the feasibility of making a laser based on nuclear transitions [4]. Even in the simplest picture, though, population inversions of the required magnitude can, in principle, be achieved only in the (radiochemical) lifetime range of hours or longer, whereas resonant absorption cross sections are generally significant only in the (Mössbauer) lifetime range of microseconds or shorter [5]. Switching from a long-lived to a short-lived state is one approach that has been suggested to meet this mismatch. However, our calculations in this paper support the general contention [4,5] that the energy conditions that are required to achieve significant population inversions are very stringent and consequently are quite incompatible with the critical requirements needed to maintain a significant stimulated emission cross section; the conditions for laser gain are conveniently listed in Ref. [6].

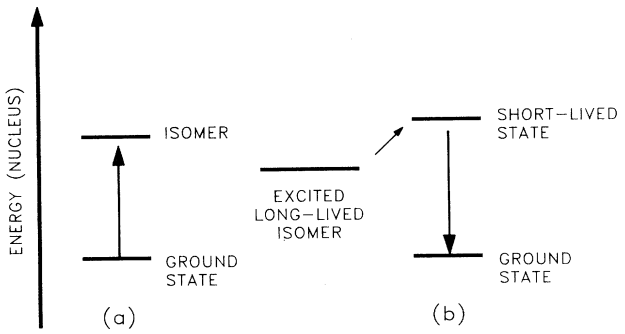

FIG. 1. Schematic diagram of the types of transitions that are of interest in laser-driven electron-nuclear excitation. These include transitions (a) from a nuclear ground state to a low-lying isomeric excited state (e.g., as in ^{235}U) and (b) from a long-lived nuclear isomeric level to a shorter-lived nuclear excited state (e.g., as in ^{110}Ag).

For each of the two aforementioned lifetime regimes, radiochemical and Mössbauer, one can consider carrying out experiments of definite physical interest. In the radiochemical regime, experiments could be performed to investigate the transition from a long-lived isomeric nuclear state to a shorter-lived nuclear excited state by detecting the rapid emission of (non stimulated) γ rays not attributable to the slower decay of the initial long-lived isomer. In the Mössbauer range, experiments could be undertaken to study the excitation of nuclei which subsequently undergo enhanced decays [7]. In the latter case, we currently believe that the number of such participating nuclei with enhanced decays will probably be quite small [8]. Although many techniques exist for the excitation of nuclei, we restrict ourselves here to the area of nuclear excitations which result from electronic motions, an aspect receiving increased attention. We note in passing that photonuclear absorption can also lead to isomeric depopulation.

The simple model which we study in this paper describes the excitation of collective nuclear rotational motion due to the motion of an electron in both the Coulomb field of the nucleus and the intense, high-

frequency field of the laser. This simple model approach seeks to identify basic aspects of the problem and to provide orders of magnitude of physical effects. Three different energy regimes of potential interest are (i) the low-energy γ-ray regime (nuclear emissions generally lower than 100 keV in energy), a regime in which no lasers currently exist (ii) the x-ray laser regime (atomic emissions generally lower than 5 keV in energy) where there are perturbations primarily to the electronic motion so that in this case energy is transferred to the nucleus by the oscillating electronic charge, and (iii) the high-intensity optical to ultraviolet (uv) photon regime where the possibility of collective electronic motions exists as well. In this paper, we will limit ourselves to some of the nuclear results that we have obtained by carrying out investigations in the x-ray regime. For comparison to the behavior in this x-ray regime, we additionally made initial investigations of the energy transfer in the γ-ray and the optical-uv regimes. The model and approach which we develop is primarily suitable for the study of the electron-nuclear interaction and energy transfer in the presence of intense laser fields, particularly in terms of its dependence on energy and intensity of the laser. Also included in our discussion will be some general comments about the availability of the laser parameters and the possibilities for observing the excitation. Since we find energy transfers in the eV to low-keV range (not MeV) the applicability is limited to low-energy nuclear transitions which do exist as also summarized later in the discussion.

II. BACKGROUND

Theoretical or model investigations of energy transfer to the nucleus by laser-driven electronic motions have been reported recently by several groups [9]. In 1985, Baldwin, Biedenharn, Rinker, and Solem addressed the energy-transfer question by focusing on the laser-electron interaction and utilizing a perturbative approach to estimate nuclear excitation probabilities [1]. On the other hand, Noid, Hartmann, and Koszykowski carried out a study of the coupled dynamics of the electron-nuclear system using a semiclassical approach [2]. Finally, Berger, Gogny, and Weiss have examined the physics of laser-driven free classical electron motion and used a perturbative approach to evaluate the nuclear matrix element [3].

In this paper we describe a simple laser-electron-nucleon model where the nucleus undergoes collective rotational motion. Previous preliminary investigations by us utilized an individual-particle model for the nuclear excitations [2], although those preliminary studies were of use in exploring the feasibility of coupled models of this general type, they had led to frequencies that were much too high to be of practical importance for low-lying nuclear states. The collective nuclear term which we consequently shall introduce into the Hamiltonian in Sec. III of this paper characterizes more realistically many of the actual low-lying states of heavy rotational nuclei. Hence, this new Hamiltonian provides a significant improvement for studying energy transfer to a nucleus of high atomic weight by laser-driven electron motions at lower frequencies. Our semiclassical approach [10] is one which solves Hamilton's dynamical equations of motion for the electron and nucleus system, starting from the initial quantum conditions, and treats the laser field classically as an explicit function of time. More details about this approach will be provided next in Sec. III.

III. MODEL

A simple model of coupled electronic and nuclear motion is used as a first step to study electronic-nuclear energy-transfer processes in the presence of a laser field. The time-dependent nuclear-electron-laser Hamiltonian $H(p,r,t)$ for this coupled system is

$$H(p,r,t)=H_n(p_n,r_n)+H_e(p_e,r_e) +H_c(r_e,r_n)+H_{\text{laser}}(r_e,r_n,t)\ , \tag{1}$$

where H_n is the nuclear term, H_e is the electronic term, H_c is the electron-nuclear coupling term, and H_{laser} is the time-dependent laser term. Here r_n represents position and p_n momentum of the nucleus, and similarly r_e and p_e for the electron. Both H_c and H_{laser} depend on r_e and r_n but not on corresponding momenta.

A. The nuclear term H_n

The nuclear Hamiltonian H_n describes the motion of a reduced mass μ_n in a potential well; it is used to treat the case of a deformed rotating nucleus with a variable moment of inertia:

$$H_n(p_n,r_n)=\mu_n c^2\left[\left[\frac{p_n^2+\mu_n^2c^2}{\mu_n^2c^2}\right]^{1/2}-1\right]+\frac{\alpha}{2r_n^2}+\frac{\beta r_n^N}{N}\ . \tag{2}$$

Here α, β, and N are parameters which describe the potential well and are explained further below. The last two terms represent an extension [11] to the variable moment of inertia (VMI) model commonly used in nuclear physics.

This choice of the nuclear term in the Hamiltonian is an improvement upon the one that was employed in our earlier investigation [2] of a preliminary model of laser-electron-nuclear energy transfer which utilized an individual-particle model for the nuclear term H_n. In that individual-particle approximation, the characteristic frequencies that are obtained, typical of nuclear excitations in nuclei near closed shells, turned out too high to be of practical interest. We noted there, though, what should be an important and general physical feature—the energy transfer between the electronic motion and nuclear motion takes place mostly during the brief time that the electron trajectory is nearest the nucleus. We find that during this brief time period, in some high-Z cases (e.g., $Z = 82$) the electron's classical velocity becomes sufficiently large so that we must use in our Hamiltonian Eq. (1), in the H_e term, the relativistic form for the electron kinetic energy. As a practical feature, then, we keep the relativistic form also in Eq. (2) above, both for the nuclear reduced mass and the kinetic energy of the nucleus, cases where it is much less important, as well as

for the single electron's kinetic energy in Eq. (4) below.

The nuclear term is intended to describe a deformed rotational nucleus. The potential well in Eq. (2) can be solved approximately, using a semiclassical approximation [11] exactly to give the nuclear energy E as a function of the nuclear spin I:

$$E(I)=\left[\frac{1}{2}+\frac{1}{N}\right]\beta^{2/(N+2)}\left[\alpha+\left[I+\frac{1}{2}\right]^2\frac{\hbar^2}{\mu_n}\right]^{N/N+2}. \tag{3}$$

The parameters α, β, and N can be fit to the rotational band spacings, as has been done [11] for a number of heavy nuclei.

B. The electronic term H_e

Our model greatly simplifies the problem by assuming that only a single electron is relevant to the process of interest. We hope to extend our work in the future to also include the possibility of collective electronic motions.

The single-particle electron term H_e in the Hamiltonian of Eq. (1) is given by

$$H_e(p_e,r_e)=mc^2\left[\left[\frac{p_e^2+m^2c^2}{m^2c^2}\right]^{1/2}-1\right]-\frac{Ze^2}{r_e}, \tag{4}$$

with energy levels

$$E=mc^2\left[1+\frac{\alpha^2Z^2}{[n_r+(K^2-\alpha^2Z^2)^{1/2}]^2}\right]^{-1/2}-mc^2. \tag{5}$$

The numbers n_r and K are the radial and quantized angular momentum quantum numbers, respectively; α is the fine-structure constant. For $\alpha Z \ll K$, the denominator becomes n^2, where the principal quantum number $n=n_r+K$. In a manner consistent with nonrelativistic quantum mechanics with spin, we let $K=j+\frac{1}{2}$. Then for $n=1$, $n_r=0$, $K=1$, and $j=\frac{1}{2}$; for $n=2$; $n_r=1$, $K=1$, $j=\frac{1}{2}$ and $n_r=0$, $K=2$, $j=\frac{3}{2}$, etc. (In the usual semiclassical approximations which treat nonrelativistic quantum mechanics with spin and deviate from the "old quantum theory," for $n=1$, $K=\frac{1}{2}$ and $n_r=\frac{1}{2}$, giving an elliptic orbit, since $n>K$. In treating the relativistic corrections in the kinetic energy term we do not need these further approximations. Alternately, we recover the approximations of "old quantum theory" when utilizing a semiclassical relativistic approach based on Sommerfeld [12] as recently highlighted by Jackson [12]).

At the outer turning point of the electron's orbit $r_{e,\max}$, we have

$$E=c\left[\frac{K^2\hbar^2}{r_{e,\max}^2}+m^2c^2\right]^{1/2}-mc^2-\frac{Ze^2}{r_{e,\max}}. \tag{6}$$

From Eq. (6), the outer turning point radial distance $r_{e,\max}$ can be found by iteration for a given E. For the purposes of our calculation, the distinction between orbital and total angular momentum is less important than ensuring that the term treating the orbital energy as given by $K^2\hbar^2/r^2$ be calculable.

C. The electron-nucleus coupling term H_c

In the absence of nuclear internal degrees of freedom, the electron moves in the Coulomb field of the net charge of Z protons. With our description of the nucleus as a simplified rotor, the electron moves in the potential well given by $(Z-k)$ "core" protons and k "valence" protons, that is, associated with the mass μ_n. The electrostatic coupling term is then given by

$$V(r_e,r_n)=-\frac{ke^2}{|r_e-r_n|}-\frac{(Z-k)e^2}{r_e}+\frac{Ze^2}{r_e}. \tag{7}$$

The last term in Eq. (7) simply corrects Eq. (4) by undoing the static nuclear term in the single-particle Hamiltonian. An electrostatic repulsive term depending on the product Zk is not included in Eq. (7) since the nuclear potential models the net effect of all the nuclear forces, including Coulombic repulsion. We ignore screening; thus our electron trajectories would characterize those of Ref. (3) except that we include those additional effects of the Coulomb potential well that are important to our model.

D. The laser term H_{laser}

The final term in the Hamiltonian H_{laser} has the explicit time dependence

$$H_{\text{laser}}=\epsilon\mu(r_e,r_n)\cos\omega t. \tag{8}$$

The quantity μ is the total system dipole moment:

$$\mu=\sum_i q_i r_i \tag{9}$$

summed over the location of all three point particles in the three-body model: the electron, the nuclear rotor reduced mass, and the core nuclear well. For convenience, we have fixed the origin of the coordinate system at the mean position of the core nucleons, specifically at the origin of the nuclear potential in which the mass μ_n moves. The quantities ϵ and ω are the electric field strengths and frequencies, respectively, of the driving laser field. The model is pictured in Fig. 2.

The complete model, thus described, is not easily solved by direct quantum-mechanical approaches. Then again, precise solutions are not needed to understand the basic behavior. One simplification, to treat the single electron as free in the electric field of the laser, allows one to calculate the nuclear transition matrix element under the perturbation of a Coulombic interaction with a sinusoidally oscillating classical electron in a linear model [3]. We have chosen to keep the complexity of the nuclear Coulombic attraction, as well as a two-dimensional (versus linear) model, in treating the electron-nuclear interaction with short-wavelength laser fields. In so doing, the classical trajectory becomes more complicated, and a simple approximation, such as a sinusoidal motion, is less appropriate. As a price, though, we have to include a relativistic treatment of the electron for inner shell electrons and an approach to calculating the energy transfer to the nucleus. The semiclassical approach, thus chosen, then proceeds along the lines of Refs. [10], [13], and [14], which exploit the use of classical trajectories computed

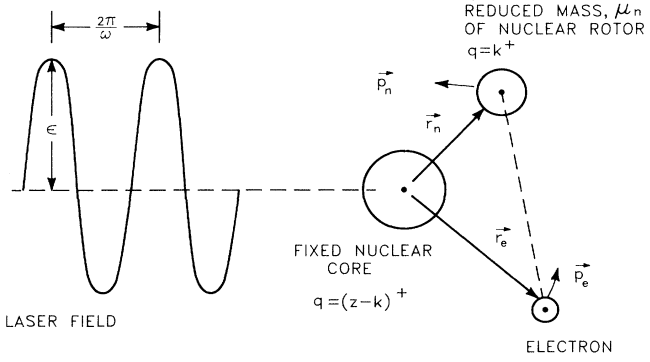

FIG. 2. The model basically describes the interaction of a three-body system with an intense laser field having intensity ϵ and frequency ω. The electron, with charge $q=-1$, interacts via the Coulomb field with the nuclear collective rotor of overall charge $+Z$; the nuclear rotor is treated as a reduced mass μ_n of charge $+k$ moving in a modified harmonic-oscillator well as parametrized in Ref. (11).

from initial quantum conditions to study the energy-transfer effects. The semiclassical approaches we use are briefly summarized.

The spectral analysis method [10] is used to obtain power spectra $I(\omega)$—with I the intensity and ω the frequency—of the dynamical variables, denoted generally by $\hat{x}(t)$. The spectral analysis method can be applied to any autocorrelation function, e.g., of coordinates $x(t)$ or $y(t)$, momenta $p_x(t)$ or $p_y(t)$, or any dynamical variable, e.g., the dipole moment $\mu(t)$. We use $\hat{x}(t)$ to denote any of these; our main interests are in the dipole moment autocorrelation function. In this approach, Hamilton's equations

$$\dot{p}=\frac{-\partial H}{\partial x}\ , \quad \dot{x}=\frac{\partial H}{\partial p}\ , \tag{10}$$

together with the proper initial conditions, are used to generate classical trajectories. The trajectories are computed using an ordinary differential equation solving computer code, described later in Sec. IV. The trajectories $\hat{x}(t)$ are then used to calculate the autocorrelation function $C(t)=\langle\hat{x}(0)\hat{x}(t)\rangle$ from which the power spectrum $I(\omega)$ is subsequently obtained by using the Fourier relationship

$$I(\omega)=\frac{1}{2\pi}\int_{-\infty}^{+\infty}C(t)\exp(-i\omega t)dt\ . \tag{11}$$

According to the Bohr correspondence principle, the mechanical frequencies ω_{mn} are related to the energy eigenvalue differences by $(E_m-E_n)\hbar$, where m and n designate any two positive integer values. The autocorrelation function $I(\omega)$ is particularly useful in identifying the absorption spectrum of the coupled spectrum and, consequently, the frequencies at which energy transfer is enhanced. The spectral analysis method provides a useful tool in studying complicated quantum systems where one is interested in learning about the qualitative behavior of the system, along with approximate numerical results, and not in finding precise solutions which in most cases would, even in principle, often lie beyond the limited sophistication of the model being employed.

Initial conditions for the trajectories of those coupled systems which do not permit the separation of variables are obtained by quantizing the action variables J_i,

$$J_i=\oint p\ dq=2\pi(n_i+\delta)\hbar\ , \tag{12}$$

where the different J_i's are obtained by integrating over topologically i independent paths; the quantities $q(\equiv q_1,q_2,\ldots,q_N)$ and $p(\equiv p_1,p_2,\ldots,p_N)$ denote the N canonically conjugate coordinates and momenta. For the electron case, the principal quantum number n in Eq. (12) is replaced by n_r+K as described previously, yielding the energy expression Eq. (5). For the nuclear Hamiltonian, the WKB method is used to numerically obtain the quantum levels and their outer turning points. The fractional term δ in Eq. (12), as described by Keller [15], is usually 0 or $\frac{1}{2}$; here it is zero.

Typically a system interacting with a sinusoidal time-dependent energy source such as a laser will pick up energy from the source until a maximum is attained and then oscillate about a mean value. During the time that the system interacts with the laser, the system's frequency can continuously change, complicating the problem. Generally, numerous trajectories are calculated with different initial starting conditions ("phases" of the system). From the analysis of these trajectories, the averaged maximum and minimum energy values can be obtained, and hence a measure of the ensembled averaged energy spread [13].

IV. CALCULATIONAL DETAILS

The model thus described in the preceding section is useful in examining electron-nucleus energy transfers in the presence of intense electromagnetic laser fields—the work here examines the application of x-ray lasers in achieving nuclear excitation, via electronic interactions.

A number of heavy nuclei are reasonably described [11] by the variable moment of inertia model that we used to obtain the energy expression in Eq. (3). Here we use the energies of the levels of the ground-state rotational band of ^{238}U to determine the parameters α, β, and N for the potential energy terms in expression Eq. (2). An investigation of a number of rotational heavy nuclei reveals some common simple features for the ground-state rotational band of this nucleus and neighboring ones; hence, the particular choice of ^{238}U is not critical, as many such nuclei have similar characteristics.

In this model, from analysis of the fitted parameters, we use

$$V(r_n)=(330\ \text{MeV fm}^2)/r_n^2+\left[0.028\frac{\text{MeV}}{\text{fm}^2}\right]r_n^2 \tag{13}$$

for the nuclear potential well as a function of the nuclear collective radial coordinate r_n. The reduced mass is $\mu_n=26.2$ in units of the proton rest mass. Interestingly,

these parameters provide a simple model which crudely characterizes the ^{238}U nucleus as a doubly magic spherical ^{208}Pb core (closed neutron $N=126$ and proton $Z=82$ shells) with an additional 20 "valence" neutrons and 10 "valence" protons outside of the closed shells, yet provide a good fit to the energy spectrum of the ground-state rotational band. This picture can be further developed by using the empirical relation for the radius of spherical nuclear matter having A nucleons:

$$r=1.2A^{1/3}\ \text{fm} . \tag{14}$$

The core radius with $A=208$ is then calculated to be 5.9 fm and the radius of the μ_n mass with $A=30$ is obtained as 3.1 fm. This analysis therefore yields 9.0 fm as the distance of the μ_n mass from the potential well center. This latter value is sufficiently close to the independent value for the potential well minimum of $r_n=10.4$ fm that is obtained by minimizing the expression in Eq. (13), suggesting the deformed, but not extended as in a dumbbell, shape.

From the WKB solution (with $\delta=0$ and the nuclear orbital term involving l taken as l^2), 39 nuclear bound states are obtained with spins ranging up to a spin of $l=16$. The nuclear ground state with oscillator quantum numbers $(n,l)=(0,0)$ is used as the initial nuclear state. In the WKB approach, quantum-mechanical levels are identified through use of the prescription given by Eq. (12).

A number of electron orbit outer turning points are individually studied to simulate the behavior of typical single electrons which lie progressively in electronic shells from $n=1$ (K) to $n=6$ (P). For each orbit, this outer turning point is obtained by using Eq. (5) to find the energy of the electronic level and then using Eq. (6) to find the initial radial distance from the nucleus. For each orbit, the effects of electron screening by electrons in lower shells can in principle be taken into account by reducing the sum nuclear charge Z by integral amounts corresponding to the total number of inner shell electrons; this is not considered at the current level of sophistication.

A summary of model parameters appears in Table I. Given the broad extent of our problem, encompassing laser fields as well as electronic and nuclear motion we find it simplest to use units of MeV and fm. The units that we employ are summarized as follows. The frequency ω is in units of inverse "time units," where one "time unit" (denoted t.u.) is the time (3.33×10^{-24} sec) for light to travel 1 Fermi. The frequency is converted to energy units of MeV by multiplying by 197 (since the quantity $\hbar c$ is equal to 197 MeV/fm). In these convenient units, $e^2=1.44$ MeV fm; $e^2/\hbar c$ is 1/137. The electric field strength (ϵ) of the laser has units of MeV$^{1/2}$/fm$^{3/2}$. In atomic units it is often useful to introduce the quantity e/a_0^2, which describes the electric field strength in terms of the Bohr radius a_0; here $e/a_0^2=4.29\times10^{-10}$ MeV$^{1/2}$/fm$^{3/2}$. We also introduce the electric field force E (MeV/fm)$=e\epsilon$ as a parameter, so that the laser power in W/cm^2 is numerically equal to $2.64\times10^{35}E^2$. (A typical value for E here, for example, is 10^{-10} MeV/fm; the magnitude of laser power is generally in the range 10^{15}–10^{20} W/cm^2).

Our calculations were carried out utilizing the following approach. Classical trajectories in momentum and coordinate space are generated from the complete Hamiltonian using Hamilton's equations [Eq. (10)]. The initial conditions for the trajectories are taken to be those of states of the separable Hamiltonian, that is, with the coupling term H_c in Eq. (1) neglected and using the WKB approximation to find the outer turning points of the re-

TABLE I. Model parameters. (See text for the definitions of these parameters.)

Nuclear parameters
Potential well: $\alpha=660$ MeV fm^2, $\beta=0.056$ MeV/fm^2, $N=2$
$\mu_n=26.2m_p$ ($m_p=938$ MeV)
Starting nuclear state: $l_n=0$, $r_n=12.22$ fm
Electron parameters
Potential well: $Z=92$, $k=10$
Electron shells (n) and outer turning points:

n	Label	E (MeV)	R (fm)
1	K	−0.132	456
2	L	−0.0342	3580
3	M	−0.0147	8790
4	N	−0.00804	16433
5	O	−0.00505	26600
6	P	−0.00346	39400
7	Q	−0.00252	53100

Laser parameters
$\omega=5\times10^{-6}$ t.u.$^{-1}$, 1 t.u. $=\frac{1}{3}\times10^{-23}$ sec
$E=1.4\times10^{-10}$ MeV/fm or 5.28×10^{15} W/cm^2.
CRAY parameters
64 parallel trajectories
ensemble length is 20×10^6 t.u. (16 laser cycles)

duced nuclear mass μ_N in the nuclear well. The outer turning points for the electron are obtained analytically by solving the single-particle relativistic Coulomb problem, using expression Eq. (4) for H_e.

Our semiclassical approach to solving the coupled problem of Eq. (1) follows Ref. (2) and is described in greater detail in Ref. (10). The trajectories that are thus obtained for the electronic and nuclear motion are then used to calculate the autocorrelation functions of the system's total dipole moment. The absorption band shape or power spectrum is then given by a Fourier transform of these autocorrelation functions, as per Eq. (11). With the laser field initially "off," the power spectrum $I(\omega)$ that is thus obtained is used to understand the basic dynamical frequencies of the electron-nucleus system.

Subsequently, to investigate energy-transfer rates with the laser field "on," Hamilton's equations are integrated for an ensemble of 64 trajectories, each with a different initial phase for the laser field, with the initial phases evenly distributed over a range of 2π radians. This procedure is followed in order to average out any unusual trajectories that may result from any specific single choice for the initial phasing of the system. These calculations are all carried out on a CRAY computer at the Oak Ridge National Laboratory. The chosen phase ensemble conveniently exploits the vector capability of this computer; the 64 trajectories are thus all computed "in parallel." A summary of the equations of motion is included in Appendix A.

V. RESULTS

For illustrative purposes, a set of electron and nuclear trajectories is shown in Fig. 3 for one of the 64 trajectories of an ensemble (over shorter time scales than those actually used in the computations). The figure depicts the x and y planar coordinates for both an electron and nuclear trajectory for equal periods of time. The electron trajectories generally describe precessing ellipses, as is well known; they do, of course, have widely varying frequencies of the motion, depending upon which orbit is used at the starting point. The nuclear trajectories describe a rotating and vibrating motion; they are similar for each run since the starting state is chosen to be the same for all runs. The rotational motion of the nuclear rotor is much slower than that of the electron's motion for the case in Fig. 3, whereas its vibrational frequency is much larger. These single trajectories are one of many, and included for illustrative purposes. An associated total system dipole moment μ is shown in Fig. 4 as a function of time for the same L-shell electron case as in Fig. 3, except for a differing time period.

In Fig. 5, we show the ensemble averaged energy transfer for the electronic energy change and the nuclear energy change with a laser in the x-ray regime at an intensity $E=1.4\times10^{-10}$ MeV/fm and a frequency of 5×10^{-6} inverse time units (t.u.$^{-1}$) or 1 keV in energy. The energy-transfer results corresponding to various starting points are depicted. The maximum and minimum of the ensemble average energy are used to fix

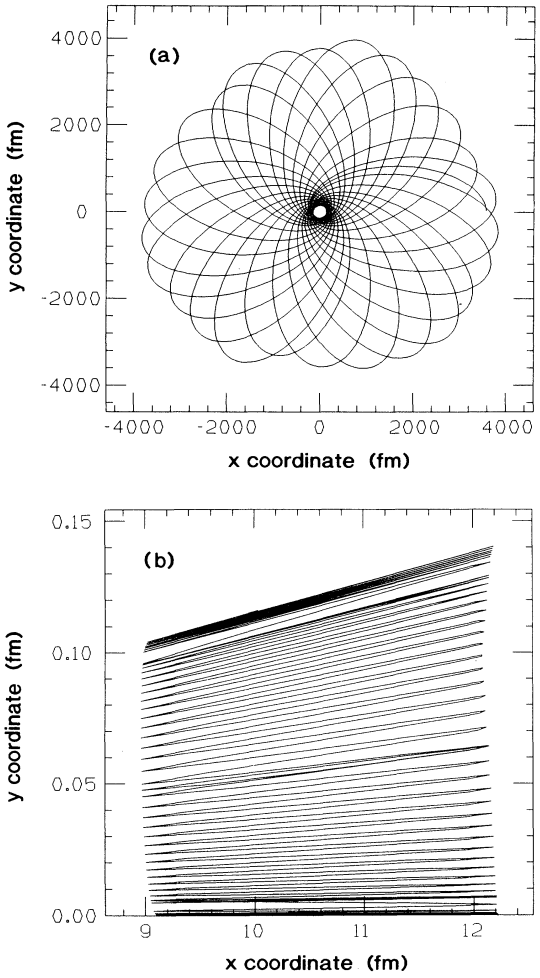

FIG. 3. Illustrative electron (a) and nuclear (b) trajectories for the L-electron ($n=2$) case in the x-ray laser field. The first 1×10^6 t.u. are shown; a complete run on the CRAY computer is actually carried out for 20×10^6 t.u. and 64 trajectories computed in parallel.

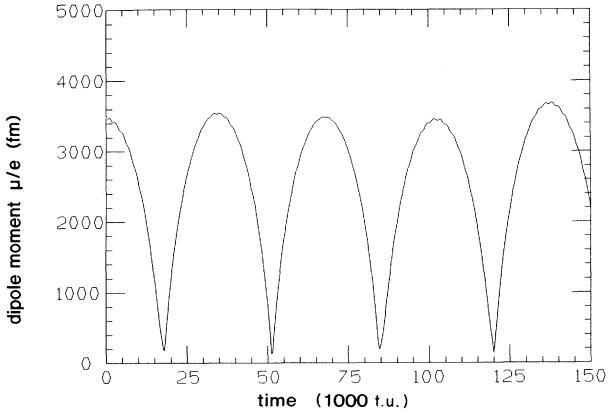

FIG. 4. Illustrative time dependence of the dipole moment for the total electron-nucleus system. This is for the L-shell case depicted in Fig. 3 and for 150 000 t.u. The dipole moment includes a large variation due to the electron motion coupled to a smaller variation due to the nuclear motion.

TABLE II. Summary of energy-transfer results.

Shell	Total electron energy change (MeV)	Total nuclear energy change (MeV)	Nuclear electron energy ratio	Nuclear excitation probability scaled per laser period[a]
K	1.2×10^{-3}	8.2×10^{-5}	0.068	0.000 18
L	6.7×10^{-3}	3.6×10^{-3}	0.54	0.007 8
M	5.0×10^{-3}	1.7×10^{-3}	0.34	0.003 7
N	3.5×10^{-3}	1.3×10^{-3}	0.37	0.002 8
O	2.6×10^{-3}	9.7×10^{-4}	0.37	0.002 1

[a]The probability, as discussed in the text (Sec. IV), is based on a semiclassical argument; it is assumed that the energy of the transition is that corresponding to the semiclassical $I=0$ state to the $I=2$ state of the nuclear rotor.

the energy-transfer values, that is, as the averaged energy spread. The electron trajectory starting points correspond to the outer turning points of orbits associated with the principal quantum numbers in the relativistic single-electron Coulomb well for $Z=92$.

The energy transfer could have been expected to increase as we go to lower and lower electron shells, reaching a maximum at the K shell in a simple model where one treats the electronic motion as totally free and hence just following the laser field. In the present work, though, as is indicated in Fig. 5, we find that the competing effects of the Coulomb field counter the strong laser electric field. This is discussed further in Sec. VI. Hence, the shells with the maximum energy transfer per electron are not the closest ones but lie further from the nuclear center. In Fig. 5, for example, the maximum energy transfer occurs for an L-shell electron. Using the energy-transfer values and assuming the excitation is entirely to the next higher nuclear quantum level, one can estimate the time-dependent excitation rate (Table II). The estimate is made by assuming that the average energy transferred leads to a state of the nucleus which is a superposition of the nucleus in its unperturbed ground and excited states. The excited state coefficient in this superposition is used to estimate the overall excitation probability which is then scaled by dividing by the number of laser cycles to obtain the excitation probability scaled per laser cycle. The above approximation is reasonably good for the relatively low probabilities of excitation per cycle which we see here in this energy and intensity regime, but it is emphasized that the energy-transfer values apply to the first 20×10^6 t.u., which is a fixed period for all runs discussed here, and no further search was yet done for nonlinear behavior of the energy at longer periods of time. (The nuclear excited state at 29 keV, $l=2$ by the WKB method was used in the estimates of the last column of Table II, and the $l=2$ degeneracy was excluded. To include the degeneracy, multiply by 5.) These results are further described in Sec. VI.

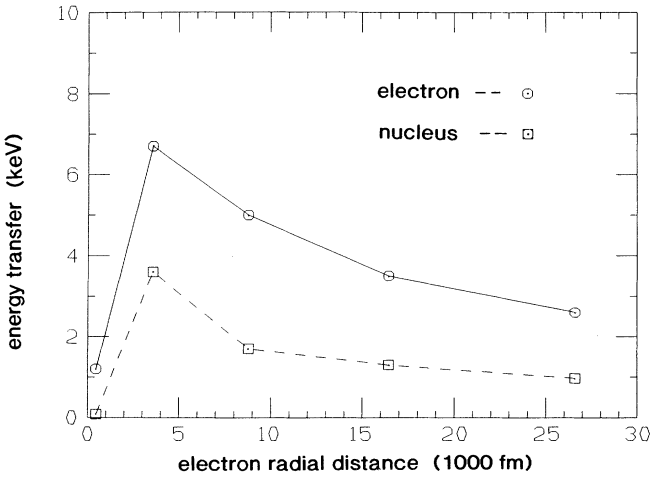

FIG. 5. Averaged electron and nuclear energy transfer as a function of the initial single-particle orbital electron outer turning point radial distance in the presence of an x-ray laser field. The circles correspond to the electron energy change and the boxes correspond to the nuclear energy change. One key feature is the drop in energy transfer at the K shell due to the competing effects of the laser-field strength and the Coulomb potential. Indeed, the maximum energy transfer occurs for an L electron, with the electron energy change larger than the nuclear energy change, as expected. This figure presents in graphical form the results that are summarized in Table II.

VI. DISCUSSION

The model studied here treats the electron-nucleus system as a three-body problem, as depicted in Fig. 2. The three bodies essentially comprise two "oscillator" systems consisting of the two-body (core-body and valence-body) nuclear "oscillator" and the electronic "oscillator." These two oscillators are independent and not notably coupled during normal circumstances, i.e., when the laser intensity is zero. With increasing laser intensity, the electronic oscillator is driven by competing effects of the usual central Coulombic field and the additional electric field of the laser [Eqs. (7) and (8), respectively]. The electron-nuclear Coulombic interaction serves as the energy transfer coupling. This basic picture of the energy-

transfer process is one which is expected to be important in laser-driven excitation of the nucleus by electronic motion. The model approach is similar to that of Refs. [10] and [13].

The results obtained with the semiclassical approach that we have employed demonstrate that the laser field has varying effects on the energy transfer, effects which depend upon both the laser intensity and the laser frequency. In this regard, the choice of a heavy nucleus to illustrate our model proves especially convenient since it permits the study of a wide range of electron orbits and their associated binding energies (see Tables I and II). From use of such a model, we find that the laser's field intensity plays a very important and surprising role—since the laser is treated as a classical electric field, even at the lowest of laser frequencies a high laser intensity results in an alteration of the electron's motion sufficient to achieve notable coupling of the electron motion to the nuclear motion.

The main focus of the applications of our model that were presented in the present paper were in the x-ray laser wavelength regime. A sequence of computer runs was performed using all the parameters of a 1-keV photon-energy laser: a frequency of 5×10^{-6} t.u.$^{-1}$ and electric field strength of 1.4×10^{-10} MeV/fm. For these laser parameters, we carried out separate studies with an electron in each of the shells from the K through O shells ($n=1$ through $n=5$, the latter being immediately subvalence). The energy-transfer results are summarized in Table II and depicted in Fig. 5.

For energy transfer in the ultrashort-wavelength regime that we studied, we would have naively guessed that the dominant contributions to nuclear excitation would be from the electrons which pass closest to the nucleus [2]. These inner-shell electrons are clearly much more bound than their outer-shell counterparts (see Table I), and therefore they would be expected to be less susceptible to being affected by the laser field. However, from our results in Table II and Fig. 5, we see that, in actuality, a balance is attained between these competing effects. The energy transfer increases as the electron moves in orbits which are located closer and closer to the effect of the nucleus from O to L until the competing effect of the Coulomb field enters significantly, thus countering the electron's radial motion. The drop in the K-shell energy transfer is clearly evident in Fig. 5.

We scale the energy transfer to the nucleus, relating it to the total energy (29 keV) needed to excite the nucleus from its ground state to a level of 29 keV (next excited rotational level in our model) and to the number of laser cycles (noted previously in Sec. V). This is a very crude measure of an excitation probability which is of use when a semiclassical model is employed. We see from Table II that measurable excitation probabilities are achieved. Our use of a collective nuclear model instead of the single-particle model which was employed in Ref. (2) results in favorable enhancements of the excitation probabilities. On the other hand, while we do take into account the nuclear Coulomb field, we still exclude the effects of electron screening. Such screening would have unfavorable effects on the excitation probabilities and would diminish the contributions of the inner electrons to nuclear excitation.

The main focus of this study is to treat the intermediate x-ray wavelength regime. Additionally, however, we explored some features at the very short and longer extremes of laser wavelengths around 1000 eV: a 5-eV very intense laser, and also a hypothetical γ-ray regime laser, for comparison with the x-ray regime results. Not unlike laser energy absorption by simple molecular oscillator studies [13], the possibility does exist even at very short wavelengths for resonances to occur at specific laser frequencies. Very high laser intensities and frequencies were therefore used to map one such resonance at a frequency of 4.4×10^{-3} t.u.$^{-1}$ (corresponding to 80 keV) and at an intensity of 1.4×10^{-6} MeV/fm. The resonance was identified by running calculations from 4.0 to 4.6×10^{-3} t.u.$^{-1}$ at laser intensities of 1.4×10^{-6}, 1.4×10^{-7}, and 1.4×10^{-8} MeV/fm, respectively. Even at such extreme conditions the enhancement factor of only 1.5 in energy transfer is not large and led us to observe that the electron-nuclear coupling was much weaker after including relativistic corrections to the K-shell trajectory. For the moment, there are no such lasers in the low-energy γ-ray regime [4], and this wavelength regime was not further pursued.

At the other extreme of laser parameters, we examined the more practical case of the low-energy, high-powered laser having a photon energy of 5 eV and a power level of 14×10^{16} W/cm^2. This corresponds to a frequency of 2.53×10^{-8} t.u.$^{-1}$ and an electric field intensity of 6.07×10^{-10} MeV/fm. Calculations at this extreme wavelength are computationally intensive due to the great disparity in the nuclear, electronic, and laser frequencies. From selected computer runs, we found that an electron in the M shell and all higher shells ($n\geq3$) photoionize before we reach the minimum time of 10^{+8} time units that we use to enable us to at least sample a half laser cycle. The successive ionization times are 4.5×10^6 t.u. for the P-shell electron, 1.1×10^7 t.u. for the O-shell electron, and 4.0×10^7 t.u. for the M-shell electron. These outer-shell electrons, then, can be treated as free in the laser field—supporting this assumption as used in the free-electron perturbative approach [3]. For the case of the L electron, which is much more tightly bound than the other outer-shell electrons in this model atom (see Table I), the electron was not observed to have ionized by the completion of the computer run which corresponds to 10^8 t.u. The energy transfer to the nucleus in this longer-wavelength optical regime in the sequence of the electron shells for P to L steadily increased. The fraction of energy transmitted to the nuclear motion scaled over a common fixed time period of 10^8 t.u., assuming once again the same model transition energy of 29 keV from the ground to first excited states, varied from 0.000 11 for the P electron to 0.000 43 for the O electron to 0.0015 for the M electron and finally to 0.50 for the L electron—a trend that is once again both consistent with the relative trends predicted by the free-electron approach and with our results in the x-ray regime. These approximate results for the transition probability are high and probably overestimate the transition

probability. This is because the semiclassical estimates that were made in this case do not distinguish the superposition of the final state amongst rotational and vibrational nuclear eigenstates, and also because of the gross simplification of one-electron models in ignoring electron screening as also emphasized in Ref. [3]. Indeed, the relatively large L-shell contribution to the Coulombic energy transfer at these lower frequencies is perhaps exacerbated due to such simplifications, although the jump increase over the P-through M-shell contributions can in part be attributed to the propensity of the latter to rapidly ionize and have less time to interact with the nucleus. (A complete treatment and discussion of this uv regime, in particular, is beyond the scope of the paper—the longer wavelength requires more computational time than does the x-ray regime for which the model is uniquely applied and more computationally tractable. Continued work in the uv region hinges on practical aspects of computations and work here is in progress.)

We can compare the magnitudes of the energy transfer in the ultrashort-wavelength laser regime with the energy transfer in the uv-optical wavelength regime. Even though electric field intensity in the x-ray case was chosen to be comparable to that for the uv-optical laser, the energy transfer in the x-ray regime actually was less than that for the L-shell optical case. This decrease can be attributed to the inverse relationship of the amplitude of the electron's motion to the laser frequency (combined with the absence of any dynamical resonance effects) and the direct importance of the intense electric field.

The intensity and energy regimes discussed in the study here highlight cases of interest in the application of our model. Some general comments about the choices and actual availability of the two laser frequencies (corresponding to 5 eV and 1 keV, respectively) and intensity ranges that are used in our calculations are thus in order. Lasers in the uv-regime (where we use a photon energy of 5 eV and a laser intensity of 14×10^{16} W/cm^2) do exist and our chosen values for the parameters characterize the parameter range for which it is feasible to explore the possibility of very-low-energy nuclear excitation experiments [3,9]. The associated electric field strength which we use to typify this energy regime is roughly one unit of e/a_0^2; a choice which lies midway in the range of $(0.01-100)e/a_0^2$. Such intensities, in which there is much continuing interest currently [17], raise questions about atomic motions themselves (let alone the nuclear excitation question). For a comparable intensity and for laser frequencies extending into the x-ray regime, perturbative approaches which neglect the Coulomb interaction on the electron's motion begin to fail [3]. This aspect has prompted us to utilize the semiclassical approach described in this paper. In this regard, it should be noted that x-ray lasers extending beyond 10 eV in energy and with powers of 5×10^{13} W/cm^2 and higher have been constructed [18], that lasers in the 1-keV range have been reportedly discussed, and that research beyond is conceivable [19]. Our second choice [16] of 1-keV photon energy, we admit, is based not on a specific laser frequency but rather on a frequency intended to characterize lasers having frequencies higher than that of the 5-eV regime but less than those envisioned in the hypothetical γ-ray laser (5–200 keV) [4,5] Our final choice of 80 keV for the photon energy happens to lie near a resonance feature in our model and is thus of mathematical interest. Coherence effects in nuclear decay have been experimentally measured for the 14-keV transition in ^{57}Fe in single-photon measurements [7] and proposed extensions to actually observe stimulated emission from ^{93m}Nb (at 30 keV) involve subtle and sensitive experiments [20]. Thus it can be observed that γ-ray lasers still pose unsolved challenges.

Although different behavior is expected between 5 and 200 keV, the 5–1000-eV regime is potentially where the nuclear excitation studies begin to be experimentally feasible. Our report here does not seek to treat a specific laser (or intense photon source) and nuclear system; however, such nuclei with the characteristics depicted in Fig. 1 do exist and it is possible to begin to study them initially with a synchrotron source [21]. The ^{235}U nucleus has a 75-eV electromagnetic transition from its ground state to an excited 26-min isomer and its excitation using an intense laser is considered to be experimentally achievable [9]. Even more striking, a transition of less than 4 eV is reported [22] in ^{229}Th and studies of this potentially excitable isomeric state are under consideration. Ironically the potential "ease" of excitation of these very low-lying nuclear states goes hand in hand with the corresponding difficulty in detecting their decay. Of particular interest then is the study of energy transfer from long-lived excited nuclear isomers to energetically near-lying shorter-lived states where the achievement of the energy transfer is signaled by the subsequent emission of a much more energetic γ ray, as we emphasized in the introduction. The two initial cases that we would suggest considering are ^{110m}Ag (900-eV transition from the isomer to the short-lived state) and ^{242m}Am (4.3 keV transition from the isomer); these transitions match well with the uv and x-ray photon spectra that are available from the National Synchrotron Light Source (NSLS) at Brookhaven National Laboratory. Further study of these aforementioned nuclei in laser fields having energies from 5 to 1000 eV is thus of further specific interest.

The experimental detection of excitations of the magnitude which we predict here in this model using an x-ray laser could perhaps be feasible; the energy-transfer values which we obtain in our calculations in this paper are significant (though, at the low-keV, not MeV, level) and excitation probabilities smaller by a few orders of magnitude for the excitation of ^{235}U using a 5-eV laser are reported as reasonably achievable in that experiment [3,23]. In any case, as emphasized from the start, our intent in this paper is to describe, examine, and discuss the basic features of our rather simple dynamical model for use in study of nuclear excitations in strong laser fields, an area for which no good quantitative theories yet exist.

Finally, let us provide here an illustration of the order of magnitude of the parameters that are involved. We can assume the same target size as in Ref. [3], that is, a gas at low pressure and a spot size characteristic of a laser beam, and thus estimate that about 3×10^7 nuclei can interact. Using one simulated laser pulse of 16 cycles

and with a probability per cycle of 0.0164 and assuming all shells except the K shell interact yields about 8×10^6 excited nuclei. This number is possibly grossly overestimated, both by our semiclassical assumptions and as a consequence of the exclusion of electron screening in our calculations. Still, with a 1% counting efficiency, it should be possible to detect 80 000 excited nuclei decaying over the course of the nuclear lifetime (assumed to be well less than a day).

Our biggest difficulty in proceeding to utilize our semiclassical model to obtain better estimates for specific nuclei of interest lies in our treatment of the nucleus itself. Whereas the electron does behave to a good approximation as an independent particle, the nuclear states can vary in character quite significantly from one nucleus to another, or even within the same nucleus. Our choice of a rotational nucleus does alleviate some of these concerns since nuclei do exhibit nearly identical rotational behaviors over wide regions of the Periodic Table. Furthermore, the motions of diatomic molecules (or any rotor for that matter) are cases for which the semiclassical methods have proven successful in studies of the dynamics of this type.

We anticipate that in future extensions of the present paper the treatment of a specific nucleus would require us to compute a transition matrix element for that particular nucleus. This could be accomplished by computing the time-dependent matrix element of the Coulombic nuclear-electron interaction between the two nuclear states of interest, where the coordinate of the electron in the interaction term would still be generated semiclassically in the presence of the intense laser field. We would speculate that a future extension of our work following an approach of the type outlined just above could perhaps yield the following two significant differences from our current semiclassical approach. First, the quantum-mechanical nuclear transition might be driven most strongly at a laser frequency which would generate a (complicated) electronic motion whose resulting frequency spectrum would contain at least one frequency component that either would match the frequency corresponding to the energy difference of the nuclear transition or else would be a multiple thereof (the semiclassical approach deals with characteristic frequencies of the motion). Second, the excitation probability will be, in the quantum-mechanical case, a true transition probability and not an average of the energy transferred. In these quantum-mechanical calculations, by still utilizing the electron's semiclassical trajectory, we would still include the non separable effects of both the central Coulombic well and the intense field of the laser, our goal as noted at the outset of our paper. In summary, the use of the semiclassical electron trajectories from our present model, in conjuction with a quantum treatment of the nucleus, would provide a more refined approach to treating specific nuclei. This extension of our model is being pursued by us.

The model approach used here has many realistic features and uses well-chosen parameters. It still suffers somewhat, however, from several aforementioned simplistic approximations, including use of the semiclassical approach and lack of electron screening. Just as it does in the case of classical trajectory studies in molecular mechanics [10], on the other hand, the semiclassical approach considered still provides insight into the major features associated with nuclear excitation by a laser-driven electron. A time-dependent Hartree-Fock approach [1] is one route to further addressing the electronic motions. As far as the absence of electron screening is concerned, all our results remain as overestimates, especially for the transition probabilities of the inner-shell electrons. Finally, extending our model to collective (rather than single-particle) electron motions will tend to increase the transition probabilities.

VII. CONCLUSION

We have been exploring the application of a semiclassical dynamical approach to energy transfer in a coupled laser-electron-nuclear system for a simple model where the collective features of a rotational nucleus are included. We report here on some of our results on the behavior of the model in the x-ray region of laser wavelengths. The behavior of the model can also be similarly explored in the uv energy regime and the γ-ray regime. Our model, having some advantages in its simplicity, is useful in understanding qualitatively the nature and some of the important features of energy transfer in nonradiatively coupled systems. Our model should also be readily adaptable to further extensions involving refinements in modeling more complicated (e.g., collective) electron motions and an improved quantum treatment of the nucleus. Such extensions, of course, are of utmost interest in this field. Preliminary results of these investigations are presented in Refs. [2] and [16].

ACKNOWLEDGMENTS

We gratefully acknowledge the support of the Division of Materials Sciences, Office of Basic Energy Sciences, U.S. Department of Energy, the National Science Foundation (Y.Y.S.), and Stockton Sabbatical, Distinguished Faculty Research, and R&PD Release Time Grants (Y.Y.S.). We additionally appreciate most helpful discussions about laser fields with Dr. S. R. Rotman of the Ben-Gurion University of the Negev in Israel. Very useful interactions with members of the Ultrashort Wavelength Laser Research Program, including Dr. H. Pilloff of the Office of Naval Research, Dr. J. Davis and Dr. P. Kepple of the U. S. Naval Research Laboratory, are gratefully acknowledged. Research sponsored by the Department of Energy at Oak Ridge is under Contract No. DE-AC05-84OR21400 with Martin Marietta Energy Systems, Inc.

APPENDIX: THE EQUATIONS OF MOTION

The approach used in this model includes the computation of the trajectories based on Hamilton's equations. The Hamiltonian, for this purpose, is a sum of four terms as described in the text:

$$H=H_n(p_n,r_n)+H_e(p_e,r_e)+H_c(r_e,r_n)+H_{\text{laser}}(r_e,r_n,t)\ . \tag{A1}$$

For the case of two objects in two dimensions, the electron e and the nuclear rotor n reduced mass μ_n, there are eight variables of interest: the position and momentum components for the electron, $r_e=(x_e,y_e)$, $p_e=(p_{x_e},p_{y_e})$ and likewise for the reduced mass treating the nuclear motion, $r_n=(x_n,y_n)$, $p_n=(p_{x_n},p_{y_n})$. Each such eight-component vector, corresponding to the positions and momenta of the two objects, itself comprises one component of an array of 64 vectors; the 64 trajectories are computed in parallel, exploiting the machine features of a CRAY XMP computer at the Oak Ridge National Laboratory. The starting point for each of the 64 trajectories is obtained from 64 points chosen uniformly in time from a trajectory propagated from one initial state of the electron-nucleus system. That state is chosen to comply with the semiclassical quantization constraint explained in the text, but with the laser-field term absent. In this way a good set of 64 starting points is obtained so that the associated 64 systems have differing phase relationships with the laser field when the trajectories are begun.

As presented in the main text, the resulting nuclear equations of motion used in the computer calculation are (all momenta p here refer to the nucleus, so the subscript n is suppressed for clarity):

$$\frac{\partial x_n}{\partial t}=\frac{\partial H}{\partial p_x}=\frac{p_x c}{(p_x^2+p_y^2+\mu_n^2c^2)^{1/2}}\ , \tag{A2}$$

$$\frac{\partial p_x}{\partial t}=-\frac{\partial H}{\partial x_n}=-\left[-\frac{\alpha}{|r_n|^3}+\beta|r_n|^{(N-1)}\right]\frac{x_n}{|r_n|} -\frac{ke^2(x_n-x_e)}{|r_e-r_n|^3}-\frac{ke\epsilon}{\sqrt{2}}\cos\omega t\ . \tag{A3}$$

The electron equations of motion are (all momenta p here refer to the electron, so the subscript e is suppressed for clarity):

$$\frac{\partial x_e}{\partial t}=\frac{\partial H}{\partial p_x}=\frac{p_x c}{(p_x^2+p_y^2+m^2c^2)^{1/2}}\ , \tag{A4}$$

$$\frac{\partial p_x}{\partial t}=-\frac{\partial H}{\partial x_e}=-\frac{(Z-k)e^2x_e}{|r_e|^3}-\frac{ke^2(x_e-x_n)}{|r_e-r_n|^3} +\frac{e\epsilon}{\sqrt{2}}\cos\omega t\ . \tag{A5}$$

The equations apply to one trajectory and one coordinate, x. The equations of motion for the y coordinate are obtained by replacing x with y; the laser field is then fixed at an angle of $\pi/4$, and it has equal components on the x and y axes. The time coordinate is treated explicitly and no derivatives are taken with respect to it. The trajectories are checked by back integration of a final point of a given trajectory in the inverse direction. The ordinary differential equation (ODE) solver is that which has been commonly used in similar semiclassical calculations [13], it is worthwhile to point out that even though a time duration is broken down into time steps, with even coarser steps used in figures, the differential equation solver chooses much smaller steps as it deems necessary by its built-in algorithms.

*Present address: Chemistry Department, Brookhaven National Laboratory, Upton, NY 11973.

†Permanent address: Stockton State College, Pomona, NJ 08240.

[1] L. C. Biedenharn, K. Boyer, and J. Solem, in *Advances in Laser Science I, University of Texas, Dallas, 1985,* Proceedings of the First International Laser Science Conference, edited by W. C. Stwalley and M. Lapp, AIP Conf. Proc. No. 146 (AIP, New York, 1986), p. 50.

[2] D. W. Noid, F. X. Hartmann, and M. L. Koszykowski, in *Advances in Laser Science II,* Proceedings of the Second International Laser Science Conference, edited by M. Lapp, W. C. Stwalley, and G. A. Kenney-Wallace, AIP Conf. Proc. No. 160 (AIP, New York, 1987), p. 69.

[3] J. F. Berger, D. Gogny, and M. S. Weiss, J. Quant. Spectrosc. Radiat. Transfer **40**, 717 (1988).

[4] G. C. Baldwin, J. C. Solem, and V. Goldanskii, Rev. Mod. Phys. **53**, 687 (1981).

[5] G. C. Baldwin and R. V. Khoklov, Phys. Today **28** (2), 32 (1975).

[6] G. C. Baldwin and M. S. Feld, J. Appl. Phys. **59**, 3665 (1986).

[7] J. P. Hannon and G. T. Trammel, Phys. Rev. **169**, 315 (1968); G. Faigel, D. P. Siddons, J. B. Hastings, P. E. Haustein, J. R. Grover, J. P. Remeika, and A. S. Cooper, Phys. Rev. Lett. **58**, 2699 (1987); U. van Burck, R. L. Mössbauer, E. Gerdau, R. Ruffer, R. Hollatz, G. V. Smirov, and J. P. Hannon, *ibid.* **59**, 355 (1987); G. T. Trammel, J. T. Hutton, and J. P. Hannon, J. Quant. Spectrosc. Radiat. Transfer **40**, 693 (1988).

[8] F. X. Hartmann, S. R. Rotman, and K. K. Garcia, J. Quant. Spectrosc. Radiat. Transfer **40**, 701 (1988); Phys. Rev. Lett. **60**, 2226 (1988).

[9] V. I. Goldanskii and V. A. Namiot, Yad. Fiz. **33**, 319 (1981) [Sov. J. Nucl. Phys. **33**, 169 (1981)]; Y. Izawa and C. Yamanaka, Phys. Lett. **88B**, 59 (1979); T. Saito, A. Shinohara, and K. Otozai, *ibid.* **92B**, 293 (1980); K. Otozai, R. Arakawa, and M. Morita, Prog. Theor. Phys. **50**, 1771 (1973); J. A. Bounds, P. Dyer, and R. C. Haight, in *Advances in Laser Science II* (Ref. [2]) p. 87.

[10] D. W. Noid, M. L. Koszykowski, and R. A. Marcus, J. Chem. Phys. **67**, 404 (1977).

[11] Y. Y. Sharon and R. A. Naumann, in Proceedings of the Conference on High-Spin Nuclear Structure and Novel Nuclear Shapes, Argonne National Laboratory, Argonne, Illinois, 1988, Argonne National Laboratory Report No. ANL-PHY-88-2, p. 266; R. A. Naumann and Y. Y. Sharon, Bull. Am. Phys. Soc. **32**, 1561 (1987).

[12] A. Sommerfeld, *Atomic Structure and Spectral Lines,* translated by H. L. Brose (Methuen, London, 1923); J. D.

Jackson, Phys. Today **40** (5) 34 (1987).
[13] D. W. Noid and J. R. Stine, Chem. Phys. Lett. **65**, 153 (1979).
[14] D. W. Noid, M. L. Koszykowski, R. A. Marcus, and J. D. MacDonald, Chem. Phys. Lett. **51**, 540 (1977).
[15] J. B. Keller, Ann. Phys. (N.Y.) **4**, 180 (1984).
[16] F. X. Hartmann, D. W. Noid, and Y. Y. Sharon, in *Advances in Laser Science IV,* Proceedings of the Fourth International Laser Science Conference on Advances in Laser Science IV, edited by James L. Cole, Donald F. Heller, Marshall Lapp, and William C. Stwalley, AIP Conf. Proc. No. 191 (AIP, New York, 1989), p. 509.
[17] Q. Su and J. H. Eberly, Phys. Rev. A **43**, 2474 (1991); N. Pont, N. R. Walet, and M. Gavrilla, Phys. Rev. Lett. **61**, 939 (1988); P. Kalman, Phys. Rev. C **39**, 2452 (1989); P. Kalman and J. Bergou, *ibid.* **34**, 1024 (1986).
[18] D. L. Matthews *et al.,* Phys. Rev. Lett. **54**, 110 (1985).
[19] Report of the Study Group on the Science and Technology of Directed Energy Weapons, Rev. Mod. Phys. Suppl. **59**, S62–64, S111 (1987); G. Chapline and L. Wood, Phys. Today, **28** (6), 40 (1975).
[20] J. R. Grover, Bull. Am. Phys. Soc. **35**, 1507 (1990).
[21] P. E. Haustein, F. X. Hartmann, J. R. Grover, R. A. Naumann, Y. Y. Sharon, D. W. Noid, R. Dean Taylor, G. R. Hoy, and J. P. Hannon (private communication).
[22] C. W. Reich and R. G. Helmer, Phys. Rev. Lett. **64**, 271 (1990), D. G. Burke, P. E. Garrett, T. Qu, and R. A. Naumann, Phys. Rev. C **42**, R499 (1990).
[23] J. C. Solem and L. C. Biedenharn, J. Quant. Spectrosc. Radiat. Transfer **40**, 707 (1988); J. A. Bounds, P. Dyer, and R. C. Haight in Ref. [9].